ACS APPLIED MATERIALS & INTERFACES

Research Article

www.acsami.org

Stable Low-Voltage Operation Top-Gate Organic Field-Effect Transistors on Cellulose Nanocrystal Substrates

Cheng-Yin Wang,[†] Canek Fuentes-Hernandez,[†] Jen-Chieh Liu,[‡] Amir Dindar,[†] Sangmoo Choi,[†] Jeffrey P. Youngblood,[‡] Robert J. Moon,[‡,§] and Bernard Kippelen*,[†]

[†]Center for Organic Photonics and Electronics (COPE), School of Electrical and Computer Engineering, Georgia Institute of Technology, Atlanta, Georgia 30332, United States

[‡]School of Materials Engineering, Purdue University, West Lafayette, Indiana 47907, United States

[§]Forest Products Laboratory, U.S. Forest Service, Madison, Wisconsin 53726, United States

Supporting Information

ABSTRACT: We report on the performance and the characterization of top-gate organic field-effect transistors (OFETs), comprising a bilayer gate dielectric of CYTOP/Al_2O_3 and a solution-processed semiconductor layer made of a blend of TIPS-pentacene:PTAA, fabricated on recyclable cellulose nanocrystal–glycerol (CNC/glycerol) substrates. These OFETs exhibit low operating voltage, low threshold voltage, an average field-effect mobility of 0.11 $cm^2/(V\ s)$, and good shelf and operational stability in ambient conditions. To improve the operational stability in ambient a passivation layer of Al_2O_3 is grown by atomic layer deposition (ALD) directly onto the CNC/glycerol substrates. This layer protects the organic semiconductor layer from moisture and other chemicals that can either permeate through or diffuse out of the substrate.

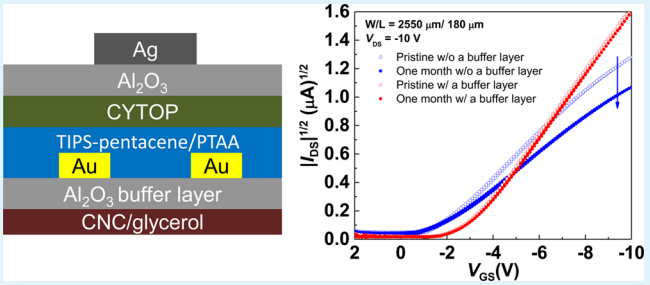

KEYWORDS: *organic field-effect transistor, top-gate geometry, cellulose, low-voltage, ambient stability*

INTRODUCTION

Because of their potential for low-cost fabrication and flexibility over large areas, organic field-effect transistors (OFETs) are important building blocks for the development of flexible electronic applications. With growing awareness of the environmental impact of electronic waste, there is a need for new substrates for emerging flexible organic printed electronic technologies with a low environmental footprint. The replacement of conventional substrates such as glass and plastics with substrates made from abundant and environmental-friendly materials can make the recycling and/or disposal of new engineered products potentially more efficient and less polluting.

Although OFETs are typically fabricated on glass or plastic substrates, paper has been the preferred substrate[1] because of its low-cost, recyclability, and use of natural materials derived from renewable feedstock. However, the fabrication of electronic components on paper presents several challenges resulting from the high porosity of traditional cellulosic materials, their high surface roughness, and complex surface chemistry. Consequently, performances of OFETs fabricated from solution on paper continue to be limited compared to of devices fabricated on glass or plastic substrates.

In recent years, cellulose nanomaterials derived from sustainable feedstock, such as cellulose nanofibers (CNFs) and cellulose nanocrystals (CNCs), have emerged as an attractive new class of materials for flexible electronic applications because they can be processed into free-standing and flexible films that display low surface roughness, good transparency, a low coefficient of thermal expansion and high thermal stability.[2] Several reports exist on organic electronic devices- such as OFETs,[3−7] organic solar cells (OPVs),[8−12] and organic light-emitting diodes (OLEDs)[13−17] fabricated on cellulose nanomaterial substrates. OFETs fabricated on CNF-based substrates have shown good flexibility and transparency,[3,4] and a majority of studies focused on processes using evaporation[5−7] and ink-jet printing.[18,19] In addition to their use as a substrate, cellulose materials were also employed as a gate dielectric[20−24] for OFETs. To date, only a few reports have demonstrated stability tests[3] and improvements are still needed in lowering the threshold voltage and increasing carrier mobility using cellulose as part of the OFETs. Solution processed OFETs containing cellulose with a low threshold voltage[25] and a high carrier mobility with environmental stability remains a goal to be achieved.

We have recently demonstrated that solution-processed OFETs with a top-gate geometry having a bilayer dielectric of CYTOP/Al_2O_3 (by atomic layer deposition, ALD) displayed

Received: December 10, 2014
Accepted: February 5, 2015
Published: February 5, 2015

DOI: 10.1021/am508723a
ACS Appl. Mater. Interfaces 2015, 7, 4804−4808

low operating voltages and excellent operational and environmental stability at ambient conditions when fabricated on glass[26,27] or plastic substrates.[28] Here, we further demonstrate that such top-gate OFETs can also be fabricated on CNC-based substrates and display low-voltage operation and good operational and environmental stability when an ALD-grown Al_2O_3 layer is used to prevent physicochemical interactions between the CNC-based substrate and the organic semiconducting layer. As we have demonstrated in the past, CNC-based substrates can easily be dissolved in water, enabling the recovery of materials after disposal of the devices.[8] OFETs fabricated on CNC with an ALD-grown Al_2O_3 buffer layer display mobility values up to 0.23 $cm^2/(V\,s)$ and are stable after 1000 cycles of transfer characteristics measurements, under DC bias stress, and show good stability at ambient conditions over a period of 16 days.

EXPERIMENTAL SECTION

Device Fabrication. OFETs were fabricated with a top-gate and bottom-contact geometry, as shown in Figure 1. CNC/glycerol substrates where prepared as described in ref 8. OFETs were fabricated on a bare CNC/glycerol substrates, referred to as D1 devices, and on a CNC/glycerol substrates coated with 300 cycles of ALD-grown Al_2O_3 at 110 °C in a Savannah 100 ALD system from Cambridge Nanotech Inc., referred to as D2 devices.

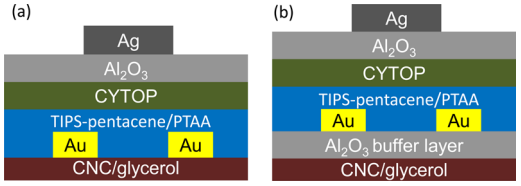

Figure 1. (a) Cross section of OFETs on bare CNC/glycerol substrates, D1. (b) Cross section of OFETs on CNC/glycerol substrates with an Al_2O_3 buffer layer, D2.

D1- and D2-type OFETs were fabricated as follows: a 2 mm-thick layer of polydimethlysiloxane (PDMS) (Gelest OE 41 with 1:1 weight ratio) was casted onto 3.8 × 3.8 cm glass substrates to hold the CNC/glycerol substrates. CNC/glycerol substrates were attached on top of the PDMS film and secured by a Kapton tape at the edges, and 50 nm-thick Au source and drain electrodes were deposited in a Denton Explorer E-beam system through a shadow mask at a deposition rate of 1.0 Å/s and at an initial pressure of 9.0×10^{-7} Torr. A TIPS-pentacene (6,13-bis(triisopropylsilylethynyl)pentacene) (Sigma-Aldrich) and PTAA (poly[bis(4-phenyl)(2,4,6-trimethylphenyl)amine]) (Sigma-Aldrich) blend solution was used as the organic semiconducting layer. A (1:1 weight ratio) TIPS-pentacene and PTAA blend solution was dissolved in 1,2,3,4-tetrahydronaphthalene anhydrous, 99%, (Sigma-Aldrich) at a concentration of 30 mg/mL. The TIPS-pentacene and PTAA blend solution was spin-coated at 500 rpm for 10 s (acceleration of 500 rpm/s) and ramped to 2000 rpm for 20 s (acceleration of 1000 rpm/s) to yield a ca. 70 nm-thick layer.[29] Spin-coated films were then annealed at 100 °C for 15 min on a hot plate in a N_2-filled glovebox. A bilayer gate dielectric was fabricated by diluting CYTOP (Asahi Glass, CTL-809M) with Asahi Glass, CTL-SOLV180 to concentration of 2% by volume. A layer of CYTOP was spin-coated on top of the organic semiconducting layer at 3,000 rpm for 60 s (acceleration of 10000 rpm/s) to yield a ca. 35 nm-thick layer.[29] Samples were then annealed at 100 °C for 10 min on a hot plate in a N_2-filled glovebox. After that, 500 cycles of ALD-grown Al_2O_3 were deposited in a Savannah 100 ALD system at 110 °C to yield a ca. 40 nm-thick layer.[29] Later, 100 nm-thick Ag gate electrodes were deposited through a shadow mask in a Spectros thermal evaporator with initial pressures below 1.0×10^{-6} Torr and at an average deposition rate of 1.0 Å/s.

Electrical Characterizations. OFET devices of types D1 and D2 were characterized in a N_2-filled glovebox (O_2 and H_2O < 0.1 ppm, 25 °C) and at ambient conditions (25 °C and 20 to 40% RH) using an Agilent E5272A source/monitor unit.

Reliability Characterizations. The operational stability was investigated by performing 1,000 continuous scans of the transfer characteristic and by applying a DC bias stress (V_{GS} = −10 V, V_{DS} = −10 V) for 60 min inside a N_2-filled glovebox (O_2, H_2O < 0.1 ppm, 25 °C) and at ambient conditions. To investigate shelf and environmental stability, devices were stored at ambient conditions and measured periodically over a period of 16 days.

RESULTS AND DISCUSSION

Electrical Characteristics. Figure 2 displays the transfer and output characteristics of selected D1- and D2-type OFETs.

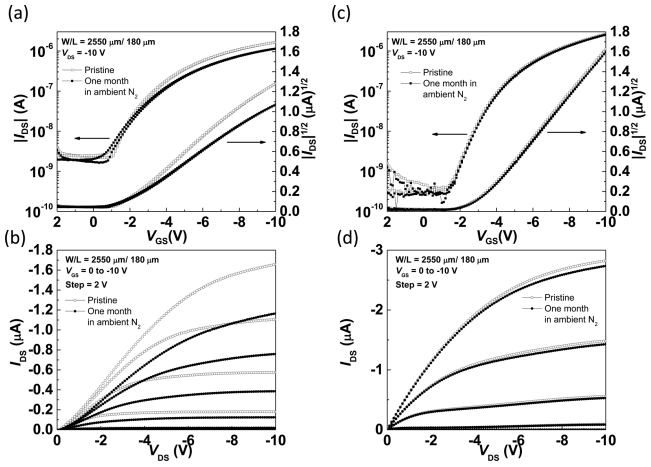

Figure 2. (a) Transfer characteristics of a D1-type OFET before and after one month in N_2. (b) Output characteristics of a D1-type OFET before and after in N_2 for 1 month. Larger current with higher V_{GS}, V_{GS} from 0 to −10 V, the step is 2 V. (c) Transfer characteristics of a D2-type OFET before and after in N_2 for 1 month. (d) Output characteristics of a D2-type OFET before and after 1 month in N_2. Larger current with higher V_{GS}, V_{GS} from 0 to −10 V, the step is 2 V.

Maximum field-effect mobility values (μ) of 0.13 $cm^2/(V\,s)$ and 0.23 $cm^2/(V\,s)$ were extracted from the transfer characteristics (in the saturation regime) of devices D1 and D2, respectively. Figure 2 also shows the transfer characteristics of the D1- and D2-type OFETs kept in N_2 for one month. In the D1 OFETs, μ decreased to a value of 0.08 $cm^2/(V\,s)$, whereas in the D2 devices, μ remained unchanged with a value of 0.23 $cm^2/(V\,s)$. The decreased mobility in the D1 devices suggests that chemical or physical interactions occur between the substrate and the organic semiconductor. However, these interactions are clearly suppressed in the D2 devices. For threshold voltages (V_{TH}) of D1- and D2-type OFETs, they do not change over 0.1 V within this time frame. Table 1 displays the average values of μ, V_{TH} and the on/off current ratio (I_{on}/I_{off}) measured in the D1- and D2-type OFETs.

To identify the chemical or physical interactions between the substrate and the organic semiconductor, we conducted X-ray photoelectron spectroscopy (XPS) measurements on bare CNC/glycerol substrates (D1′) and CNC substrates with an ALD-grown Al_2O_3 buffer layer (D2′). Figure 3 displays the binding energy spectra measured by XPS, wherein clear differences are observed between the spectra obtained for the two substrates. First, Al 2p and Al 2s peaks are detected on D2′ because of the Al_2O_3 buffer layer deposited by ALD. More

DOI: 10.1021/am508723a
ACS Appl. Mater. Interfaces 2015, 7, 4804−4808

Table 1. Device Dimensions, Average Mobility, Average Threshold Voltage, and Average on/off Current Ratio of OFETs

label	buffer layer	measurement time	W/L	C_{in} (nF/cm^2)	μ (cm^2/(V s))	ave. % change of μ	V_{TH}(V)	I_{on}/I_{off}
D1	none	pristine in N_2	2550 μm/180 μm (6/6 devices)	31.0	0.06 (±0.03)	N/A	−1.0 (±0.4)	4.8×10^2
		after 1 month in N_2		31.0	0.06 (±0.02)	−7.2	−0.8 (±0.4)	5.8×10^2
		6 days at ambient conditions		31.0		See Note		
D2	300 cycles of ALD Al_2O_3	pristine in N_2	2550 μm/180 μm (8/8 devices)	31.0	0.11 (±0.08)	N/A	−2.1 (±0.7)	2.4×10^3
		after 1 month in N_2		31.0	0.11 (±0.08)	−2.8	−2.2 (±0.7)	2.7×10^3
		16 days at ambient conditions		31.0	0.17 (±0.12)	45.1	−0.3 (±0.4)	2.2×10^2

Note: OFETs from D1 after 6 days at ambient conditions were not stable. The measured curve changed after every scanning, and it did not follow the square law so μ and V_{TH} cannot be extracted. The representative characteristic is in Figure S2 (Supporting Information) and the on/off ratio is at the range of 1 to 10. Therefore, there is no statistical data in Table 1 for D1 after 6 days at ambient conditions.

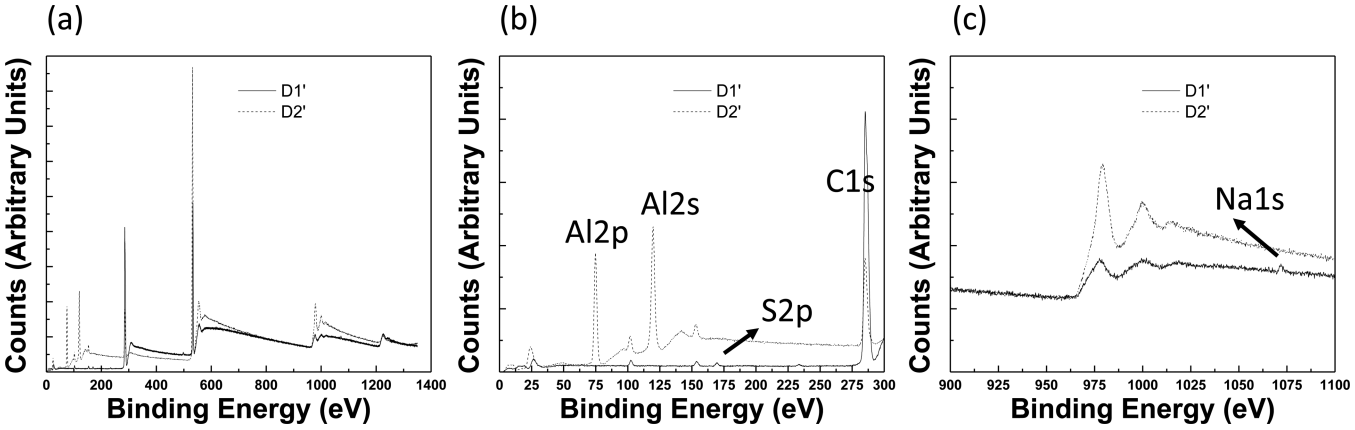

Figure 3. Binding energy spectra from XPS of a bare CNC/glycerol (D1′) substrate and a CNC/glycerol (D2′) substrate with ALD-grown Al_2O_3. (a) Binding energy from 0 to 1400 eV. (b) Zoomed-in 0 to 300 eV region of binding energy. (c) Zoomed-in 900 to 1100 eV region of binding energy.

notably, sulfur and sodium peaks are detected on D1′, but are not on D2′. The presence of sulfur suggests that sulfate half-esters are present on the surface of the CNCs/glycerol substrates as a result of the sulfuric acid hydrolysis process used for the CNC production. Sulfate half-esters hydrolyzed by water during casting of the CNC/glycerol film could produce negatively charged sulfates that would act as hole traps, which may explain the decreased mobility values observed in D1 devices after being stored in N_2 for 1 month, as shown in Figure 2, thus eliminating the possibility that these effects could be due to oxygen or water from the ambient. In contrast, the mobility displayed by D2 devices stored under the same conditions remained unchanged, as shown in Figure 2. On the other hand, the presence of sodium on the surface of the CNC substrate suggests the presence of sodium cations which may be very mobile and could lead to an increased channel conductivity. However, in pristine devices, the off current in both types of devices originates from the gate-to-drain leakage current, as displayed in Figure S1a,c (Supporting Information). The slightly larger values of gate-to-drain leakage currents in D1 devices therefore indicate that the quality of the bilayer gate-dielectric and semiconductor layers is affected by the direct fabrication of top-gate OFETs on bare CNC/glycerol substrates. The presence of sodium is an unintended consequence of the addition of glycerol to the CNC films, which improves its mechanical properties. Furthermore, we have to keep in mind that glycerol is a dipolar molecule that may be mobile, and as such, could affect the threshold voltage values[30] and operational stability of devices directly fabricated on CNC/glycerol substrates. In summary, the improved shelf stability, under N_2, and performance characteristics displayed by D2 devices, as compared to D1 devices, arises from the passivation of the chemical species present on the CNC/glycerol surface that results from the deposition of the Al_2O_3 buffer layer. In the following section, we will show that the presence of this passivation layer has further consequences for the environmental and operational reliability of top-gate OFETs.

Environmental and Operational Reliability. Figure 4 displays the results of scanning 1000 times as many transfer characteristics on both the D1- and D2-type OFETs inside a N_2-filled glovebox and at ambient conditions. D1 devices display two distinctive effects in both environments: (1) a reduction in the magnitude of the threshold voltage and (2) an increased off-current. As displayed in Figure S1b (Supporting Information), the increased off-current is not attributed to an increased gate-to-drain leakage current but to an increased channel conductivity which probably arises from the diffusion of sodium cations upon device operation. On D2 devices, the off-current increase is greatly suppressed, particularly in air, and variations of the transfer characteristics are primarily associated with smaller reductions in the magnitude of the threshold voltage than the ones observed in D1 devices. Hence, the presence of the Al_2O_3 buffer layer avoids the increase of the channel conductance and leads to more stable transfer characteristics on D2 devices than on D1 devices, in both N_2

DOI: 10.1021/am508723a
ACS Appl. Mater. Interfaces 2015, 7, 4804−4808

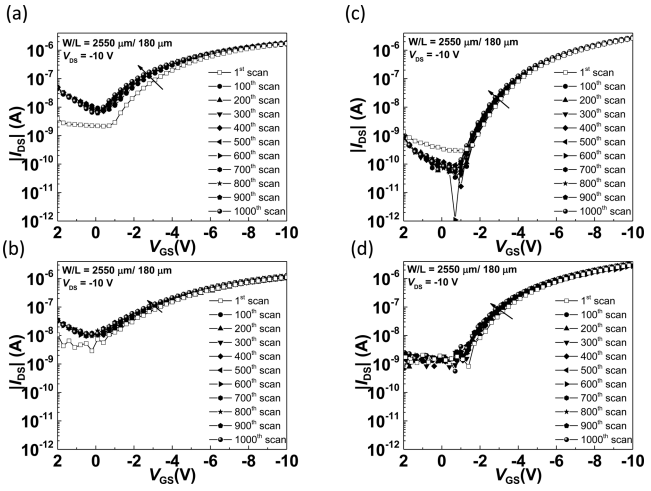

Figure 4. (a) 1000 cycles of transfer characteristics measured in N_2 on the D1-type OFET. (b) 1000 cycles of transfer characteristic measured in ambient conditions on the D1-type OFET. (c) 1000 cycles of transfer characteristics measured in N_2 on the D2-type OFET. (d) 1000 cycles of transfer characteristics measured at ambient conditions on the D2-type OFET.

and ambient conditions. This can further be seen in the evolution of the carrier mobility, V_{TH} and the on/off current ratio (I_{on}/I_{off}) values, which are extracted and summarized in Figure S2 (Supporting Information).

To further investigate the operational stability of D1- and D2-type OFETs in N_2 and ambient conditions, DC bias stress tests were also carried on the same devices for 1h. V_{DS} and V_{GS} were both biased at −10 V. Figure S3 (Supporting Information) shows that after 1 h of biasing under these conditions, the source-to-drain current of both devices increased. Consistent with the relative reductions in the magnitude of the threshold voltage observed in cycling experiments, D1 devices display a higher increase in the source-to-drain current than D2 devices, in both N_2 and ambient conditions. As we have discussed in the past,[26] the increase in threshold voltage values observed (here primarily reflected as reductions in its magnitude, see Figure S2, Supporting Information) is consistent with the presence of mobile dipoles, such as glycerol, which have a stronger effect in D1 devices than in D2 devices.

Finally, shelf environmental stability tests of D1 and D2 were conducted. Figure S4 (Supporting Information) shows electrical characteristics of D1- and D2-type OFETs stored at ambient conditions. The off-current in D1 OFETs increased 1000 times to the same level as on-current within 6 days. Meanwhile, the off-current of D2 OFETs increased only 100 times after 16 days at ambient conditions. This indicates that the Al_2O_3 buffer layer also improves the shelf environmental stability of OFETs on CNC/glycerol substrates, and provides a route toward optimizing the stability of these types of OFETs. The performance of D2 devices is comparable to the performance of OFETs with identical geometry fabricated on glass[26,27] or plastic substrates. Recently, we related the increased off-current values in top-gate OFETs fabricated on glass to an increased channel conductivity due to *p*-doping induced by diffused oxygen.[27] On the other hand, we should note that previous reports of OFETs on CNC substrates have used bottom-gate geometries.[3,7] Although the environmental and operational stability of such OFETs has not been discussed in detail, we expect the substrate chemistry to play a less important role than what we have found in this study since the use of a bottom-gate and gate dielectric layer will effectively passivate the surface of the substrate; although the substrate will likely still be permeable to oxygen and water from the environment. We have to keep in mind that a bottom-gate geometry exposes the semiconductor channel directly to the environment and, consequently, is expected to generally lead to OFETs that are less stable in ambient conditions than top-gate OFETs, including the ones presented in this work.

CONCLUSIONS

We have demonstrated top-gate OFETs on CNC/glycerol substrates with a solution-processed semiconductor layer that operate at low voltages with good shelf and operational stability. We have found that the key to achieve top-gate OFETs with stable characteristics is to isolate the organic semiconductor layer from the chemical species in the substrate. We have achieved that by deposition of a thin layer of Al_2O_3 grown by ALD, which is also clearly shown to lead to much improved environmental stability. Although the thickness and barrier properties of this layer can be further optimized, our results show that such barrier will be needed to achieve OFETs with stable performance when fabricated on substrates with poor oxygen and water barrier properties.

ASSOCIATED CONTENT

Supporting Information

Gate leakage current measurements, extracted mobility values, threshold voltage values, on/off current ratio values from Figure 4. Turn-on DC bias stress measurements measured in both N_2 and at ambient conditions on OFETs from D1 and D2, and stability tests for OFETs at ambient conditions. This material is available free of charge via the Internet at http://pubs.acs.org.

AUTHOR INFORMATION

Corresponding Author

*B. Kippelen. E-mail: kippelen@gatech.edu.

Author Contributions

The paper was written through contributions of all authors. All authors have given approval to the final version of the paper.

Notes

The authors declare no competing financial interest.

ACKNOWLEDGMENTS

This research was funded in part USDA-Forest Service (Grant No. 11-JV-11111129-118). We thank Dr. Alan Rudie from the USDA Forest Product Laboratory (FRL), Madison, WI, for providing the CNC materials.

REFERENCES

(1) Tobjork, D.; Osterbacka, R. Paper Electronics. *Adv. Mater.* **2011**, *23*, 1935−1961.

(2) Moon, R. J.; Martini, A.; Nairn, J.; Simonsen, J.; Youngblood, J. Cellulose Nanomaterials Review: Structure, Properties and Nanocomposites. *Chem. Soc. Rev.* **2011**, *40*, 3941−3994.

(3) Fujisaki, Y.; Koga, H.; Nakajima, Y.; Nakata, M.; Tsuji, H.; Yamamoto, T.; Kurita, T.; Nogi, M.; Shimidzu, N. Transparent Nanopaper-based Flexible Organic Thin-Film Transistor Array. *Adv. Funct. Mater.* **2014**, *24*, 1657−1663.

(4) Huang, J.; Zhu, H. L.; Chen, Y. C.; Preston, C.; Rohrbach, K.; Cumings, J.; Hu, L. B. Highly Transparent and Flexible Nanopaper Transistors. *ACS Nano* **2013**, *7*, 2106−2113.

DOI: 10.1021/am508723a
ACS Appl. Mater. Interfaces 2015, 7, 4804−4808

(5) Zschieschang, U.; Yamamoto, T.; Takimiya, K.; Kuwabara, H.; Ikeda, M.; Sekitani, T.; Someya, T.; Klauk, H. Organic Electronics on Banknotes. *Adv. Mater.* **2011**, *23*, 654−658.
(6) Peng, B.; Chan, P. K. L. Flexible Organic Transistors on Standard Printing Paper and Memory Properties Induced by Floated Gate Electrode. *Org. Electron.* **2014**, *15*, 203−210.
(7) Zocco, A. T.; You, H.; Hagen, J. A.; Steckl, A. J. Pentacene Organic Thin-Film Transistors on Flexible Paper and Glass Substrates. *Nanotechnology* **2014**, *25*, 094005.
(8) Zhou, Y.; Fuentes-Hernandez, C.; Khan, T. M.; Liu, J. C.; Hsu, J.; Shim, J. W.; Dindar, A.; Youngblood, J. P.; Moon, R. J.; Kippelen, B. Recyclable Organic Solar Cells on Cellulose Nanocrystal Substrates. *Sci. Rep.* **2013**, *3*, 1536.
(9) Zhou, Y.; Khan, T. M.; Liu, J.-C.; Fuentes-Hernandez, C.; Shim, J. W.; Najafabadi, E.; Youngblood, J. P.; Moon, R. J.; Kippelen, B. Efficient Recyclable Organic Solar Cells on Cellulose Nanocrystal Substrates with a Conducting Polymer Top Electrode Deposited by Film-Transfer Lamination. *Org. Electron.* **2014**, *15*, 661−666.
(10) Kim, T. S.; Na, S. I.; Kim, S. S.; Yu, B. K.; Yeo, J. S.; Kim, D. Y. Solution-Processible Polymer Solar Cells Fabricated on a Papery Substrate. *Phys. Status Solidi RRL* **2012**, *6*, 13−15.
(11) Hübler, A.; Trnovec, B.; Zillger, T.; Ali, M.; Wetzold, N.; Mingebach, M.; Wagenpfahl, A.; Deibel, C.; Dyakonov, V. Printed Paper Photovoltaic Cells. *Adv. Energy Mater.* **2011**, *1*, 1018−1022.
(12) Wang, F.; Chen, Z.; Xiao, L.; Qu, B.; Gong, Q. Papery Solar Cells Based on Dielectric/Metal Hybrid Transparent Cathode. *Sol. Energy Mater. Sol. Cells* **2010**, *94*, 1270−1274.
(13) Najafabadi, E.; Zhou, Y. H.; Knauer, K. A.; Fuentes-Hernandez, C.; Kippelen, B. Efficient Organic Light-Emitting Diodes Fabricated on Cellulose Nanocrystal Substrates. *Appl. Phys. Lett.* **2014**, *105*, 063305.
(14) Purandare, S.; Gomez, E. F.; Steckl, A. J. High Brightness Phosphorescent Organic Light Emitting Diodes on Transparent and Flexible Cellulose Films. *Nanotechnology* **2014**, *25*, 094012.
(15) Zhu, H.; Xiao, Z.; Liu, D.; Li, Y.; Weadock, N. J.; Fang, Z.; Huang, J.; Hu, L. Biodegradable Transparent Substrates for Flexible Organic-Light-Emitting Diodes. *Energy Environ. Sci.* **2013**, *6*, 2105−2111.
(16) Ummartyotin, S.; Juntaro, J.; Sain, M.; Manuspiya, H. Development of Transparent Bacterial Cellulose Nanocomposite Film as Substrate for Flexible Organic Light Emitting Diode (OLED) display. *Ind. Crops Prod.* **2012**, *35*, 92−97.
(17) Yoon, D.-Y.; Kim, T.-Y.; Moon, D.-G. Flexible Top Emission Organic Light-Emitting Devices Using Sputter-Deposited Ni Films on Copy Paper Substrates. *Curr. Appl. Phys.* **2010**, *10*, e135−e138.
(18) Bollström, R.; Määttänen, A.; Tobjörk, D.; Ihalainen, P.; Kaihovirta, N.; Österbacka, R.; Peltonen, J.; Toivakka, M. A Multilayer Coated Fiber-based Substrate Suitable for Printed Functionality. *Org. Electron.* **2009**, *10*, 1020−1023.
(19) Andersson, P.; Nilsson, D.; Svensson, P. O.; Chen, M.; Malmström, A.; Remonen, T.; Kugler, T.; Berggren, M. Active Matrix Displays Based on All-Organic Electrochemical Smart Pixels Printed on Paper. *Adv. Mater.* **2002**, *14*, 1460−1464.
(20) Pereira, L.; Gaspar, D.; Guerin, D.; Delattre, A.; Fortunato, E.; Martins, R. The Influence of Fibril Composition and Dimension on the Performance of Paper Gated Oxide Transistors. *Nanotechnology* **2014**, *25*, 094007.
(21) Gaspar, D.; Fernandes, S. N.; de Oliveira, A. G.; Fernandes, J. G.; Grey, P.; Pontes, R. V.; Pereira, L.; Martins, R.; Godinho, M. H.; Fortunato, E. Nanocrystalline Cellulose Applied Simultaneously as the Gate Dielectric and the Substrate in Flexible Field Effect Transistors. *Nanotechnology* **2014**, *25*, 094008.
(22) Petritz, A.; Wolfberger, A.; Fian, A.; Irimia-Vladu, M.; Haase, A.; Gold, H.; Rothländer, T.; Griesser, T.; Stadlober, B. Cellulose as Biodegradable High-k Dielectric Layer in Organic Complementary Inverters. *Appl. Phys. Lett.* **2013**, *103*, 153303.
(23) Valentini, L.; Bittolo Bon, S.; Cardinali, M.; Fortunati, E.; Kenny, J. M. Cellulose Nanocrystals Thin Films as Gate Dielectric for Flexible Organic Field-Effect Transistors. *Mater. Lett.* **2014**, *126*, 55−58.
(24) Thiemann, S.; Sachnov, S. J.; Pettersson, F.; Bollström, R.; Österbacka, R.; Wasserscheid, P.; Zaumseil, J. Cellulose-based Ionogels for Paper Electronics. *Adv. Funct. Mater.* **2014**, *24*, 625−634.
(25) Kawahara, J.; Andersson Ersman, P.; Wang, X.; Gustafsson, G.; Granberg, H.; Berggren, M. Reconfigurable Sticker Label Electronics Manufactured from Nanofibrillated Cellulose-based Self-Adhesive Organic Electronic Materials. *Org. Electron.* **2013**, *14*, 3061−3069.
(26) Hwang, D. K.; Fuentes-Hernandez, C.; Kim, J.; Potscavage, W. J., Jr.; Kim, S. J.; Kippelen, B. Top-Gate Organic Field-Effect Transistors with High Environmental and Operational Stability. *Adv. Mater.* **2011**, *23*, 1293−8.
(27) Hwang, D. K.; Fuentes-Hernandez, C.; Fenoll, M.; Yun, M.; Park, J.; Shim, J. W.; Knauer, K. A.; Dindar, A.; Kim, H.; Kim, Y.; Kim, J.; Cheun, H.; Payne, M. M.; Graham, S.; Im, S.; Anthony, J. E.; Kippelen, B. Systematic Reliability Study of Top-Gate p- and n-Channel Organic Field-Effect Transistors. *ACS Appl. Mater. Interfaces* **2014**, *6*, 3378−86.
(28) Hwang, D. K.; Dasari, R. R.; Fenoll, M.; Alain-Rizzo, V.; Dindar, A.; Shim, J. W.; Deb, N.; Fuentes-Hernandez, C.; Barlow, S.; Bucknall, D. G.; Audebert, P.; Marder, S. R.; Kippelen, B. Stable Solution-Processed Molecular n-Channel Organic Field-Effect Transistors. *Adv. Mater.* **2012**, *24*, 4445−50.
(29) Choi, S.; Fuentes-Hernandez, C.; Yun, M.; Dindar, A.; Khan, T. M.; Wang, C.-Y.; Kippelen, B. Organic Field-Effect Transistor Circuits Using Atomic Layer Deposited Gate Dielectrics Patterned by Reverse Stamping. *Org. Electron.* **2014**, *15*, 3780−3786.
(30) Possanner, S. K.; Zojer, K.; Pacher, P.; Zojer, E.; Schürrer, F. Threshold Voltage shifts in Organic Thin-Film Transistors Due to Self-Assembled Monolayers at the Dielectric Surface. *Adv. Funct. Mater.* **2009**, *19*, 958−967.

DOI: 10.1021/am508723a
ACS Appl. Mater. Interfaces 2015, 7, 4804−4808